Pure Appl. Chem., Vol. 80, No. 10, pp. 2151–2161, 2008.
doi:10.1351/pac200880102151
© 2008 IUPAC

Approaches to low-bandgap polymer solar cells: Using polymer charge-transfer complexes and fullerene metallocomplexes*

Sergey A. Zapunidy[1], Dmitry S. Martyanov[1], Elena M. Nechvolodova[2], Marina V. Tsikalova[3], Yuri N. Novikov[3], and Dmitry Yu. Paraschuk[1,‡]

[1]International Laser Center and Faculty of Physics, M. V. Lomonosov Moscow State University, 119991 Moscow, Russia; [2]N. N. Semenov Institute of Chemical Physics, RAS, ul. Kosygina 4, 119991 Moscow, Russia; [3]A. N. Nesmeyanov Institute of Organoelement Compounds, RAS, ul. Vavilova 28, 119991 Moscow, Russia

Abstract: Polymer solar cells have shown high potential to convert solar energy into electricity in a cost-effective way. One of the basic reasons limiting the polymer solar cell efficiency is insufficient absorption of the solar radiation by the active layer that limits the photocurrent. To increase the photocurrent, one needs low-bandgap materials with strong absorption below 2 eV. In this work, we study two types of low-bandgap materials: ground-state charge-transfer complexes (CTCs) of a conjugated polymer, MEH-PPV (poly[2-methoxy-5-(2'-ethylhexyloxy)-1,4-phenylenevinylene]), and an exohedral metallocomplex of fullerene, (η^2-C_{60})IrH(CO)[(+)DIOP] (IrC_{60}). We demonstrate that the CTC formed between MEH-PPV and conjugated molecules with high electron affinity, namely, 2,4,7-trinitrofluorenone (TNF) and 1,5-dinitroantraquinone (DNAQ), can have strong optical absorption extending down to the near infrared. We have observed that the photoexcited CTC can generate free charges. We also report on optical studies of IrC_{60} as a possible acceptor for polymer/fullerene solar cells. IrC_{60} strongly absorbs in the visible spectral range, in particular in the red part, and therefore has a potential for increasing the photocurrent as compared with polymer/methanofullerene solar cells. Our studies of MEH-PPV/IrC_{60} blended films show that long-lived charges are efficiently generated at MEH-PPV upon photoexcitation of the blend.

Keywords: solar cells; conjugated polymers; exohedral metallofullerenes; charge-transfer complex; charge generation and transport.

INTRODUCTION

Blends of conjugated polymers and fullerenes are intensively studied as promising materials for the active layer of organic solar cells. The solar energy conversion efficiency 4–6 % for the best polymer/fullerene solar cells has been reported [1–5]. Among the most efficient material combinations are blends of MDMO-PPV (poly[2-methoxy-5-(3,7-dimethyloctyloxy)-*p*-phenylenevinylene]) or P3HT

*Paper based on a presentation at the International Conference and Exhibition "Molecular and Nanoscale Systems for Energy Conversion" (MEC-2007), 1–3 October 2007, Moscow, Russia. Other presentations are published in this issue, pp. 2069–2161.
‡Corresponding author

(poly[3-hexylthiophene]) with PCBM [(6,6)-phenyl-C61-butyric acid methyl ester] (Fig. 1). The optical gap of PPV- and PT-type polymers is about 2 eV; therefore, a major part of the solar energy spectrum cannot be absorbed by the polymer that limits the photocurrent and hence the solar cell efficiency. Because of this, development of low-bandgap conjugated polymers is one of the main strategies for optimization of polymer/fullerene solar cells [5–7].

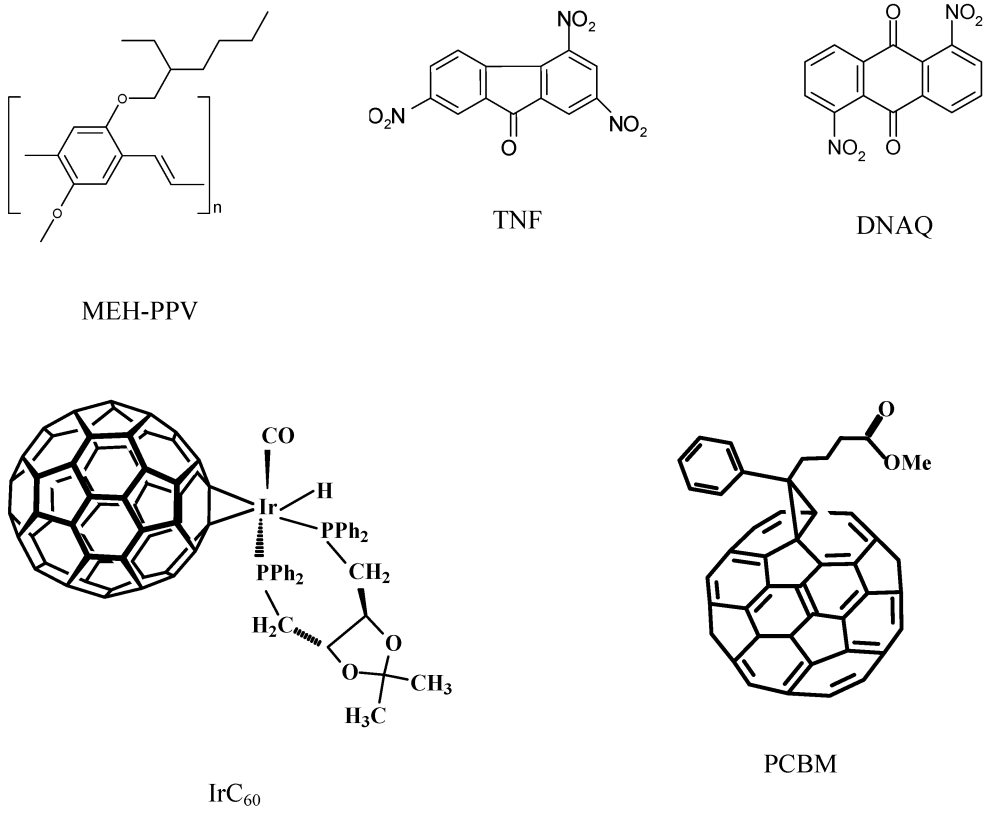

Fig. 1 Structural formulas of materials.

On the other hand, to extend optical absorption of conjugated polymer materials into the red and near-IR ranges, one could exploit the properties of donor–acceptor charge-transfer complexes (CTCs). As is well known for small π-conjugated molecules, they can easily form donor–acceptor CTCs in the electronic ground state [8,9]. These CTCs usually have a characteristic absorption band in the optical gap of both the donor and the acceptor. As was shown recently, relatively large π-conjugated molecules such as fullerenes also form CTCs with small molecules such as dimethylaniline [10], amines [11,12], and a relatively large molecule such as phthalocyanine [13]. Nonconjugated polymers can form ground-state donor–acceptor CTCs as well, e.g., the CTC between polyvinylcarbazole and 2,4,7-trinitrofluorenone (TNF) (Fig. 1) has been thoroughly studied since the 1970s as a photoconductor with sensitivity in the visible spectral range [14,15]. Intramolecular CTCs of a conjugated polymer have recently been reported for polythiophene [16], where weak charge transfer occurs within the polymer unit cell, including a covalently bound acceptor molecule.

Nevertheless, intermolecular CTCs of conjugated polymers were far less studied. There were reports on CTCs of oligothiophenes and oligoparaphenylenes with tetracyanoquinodimethane (TCNQ) [17,18], and M. S. A. Abdou et al. [19] reported on a reversible CTC between P3HT and molecular oxy-

gen. We have recently demonstrated that MEH-PPV (poly[2-methoxy-5-(2'-ethyl-hexyloxy)-1,4-phenylenevinylene]) (Fig. 1) can form an intermolecular ground-state CTC with low-molecular organic acceptors, specifically with TNF [20–23]. The MEH-PPV/TNF blend considerably absorbs in the red and near-IR ranges, resulting in generation of mobile charges [20]. These studies suggest that the ground-state CTC is involved in the photophysics of the blend, especially energy transfer and charge generation. Moreover, the ground-state CTC influences donor–acceptor phase separation in the blend [24] and therefore the blend morphology. In turn, the latter has been recognized to be of great importance for the photophysics and charge transport [25]. Moreover, it seems that ground-state charge transfer in conjugated polymer/acceptor blends is a more general feature than was thought previously. Specifically, Panda et al. [26] recently reported on CTC absorption between various conjugated polymers/oligomers and organic acceptor molecules in solution. Moreover, blends of conjugated polymers with fullerenes were intensively studied in the last 15 years, and it was generally accepted that charge transfer occurs only in the excited state of the blend but not in its ground state. However, recent studies have shown evidence of a weak ground-state CTC in blends of several conjugated polymers with PCBM [27–29]. In fact, CTC absorption in polymer/fullerene blends is quite weak, and it was difficult to identify it in the blend absorption spectrum.

At the same time, much less attention has been paid to optimization of the fullerene properties for polymer/fullerene solar cells although the PCBM content in the blend should be between 50 and 80 % by weight for the most efficient cells [2,5,25]. Much work has been done in studies of methanofullerenes, including higher fullerenes C_{70} and C_{84} [30–34]. However, despite stronger optical absorption of C_{70} and C_{84} derivatives in the optical gap of the polymer as compared with that of C_{60}, the performance of the corresponding solar cells was below that of the best polymer/PCBM solar cells. On the other hand, exohedral metal complexes of fullerenes [35] could be new interesting acceptors for polymer/fullerene solar cells. For example, $(\eta_2\text{-}C_{60})[ML_2]_n$ (M = Pd, Pt; L = ligand; n = 1,4) show considerably stronger absorption in the visible range as compared with C_{60} [36], and their lowest unoccupied molecular orbitals (LUMOs) can be significantly higher than that of C_{60} as suggested from the electrochemistry data [37]. Enhanced absorption and higher LUMO energies of metallofullerenes allow us to expect that using them in polymer/fullerene solar cells could improve their performance. In addition, metallofullerenes can have high solubility due to appropriate ligands.

In this work, to increase the photosensitivity of polymer solar cells below 2 eV, we study MEH-PPV/acceptor blends with two types of acceptors: 1,5-dinitroantraquinone (DNAQ) and TNF, forming a strongly absorbing ground-state CTC with MEH-PPV, and recently synthesized fullerene metallocomplex $(\eta_2\text{-}C_{60})$IrH(CO)[(+)DIOP] (IrC_{60}) (Fig. 1) [38], showing considerable optical absorption below 2 eV. To probe the excited states of the materials, we use optical absorption, photoluminescence (PL), photoinduced absorption (PIA), and photocurrent spectroscopies.

SAMPLES AND EXPERIMENTAL DETAILS

Figure 1 shows structural formulas of materials studied. MEH-PPV (Sigma-Aldrich) was typically dissolved in chlorobenzene or cyclohexanone at concentration 2–5 g/l for 30–180 min at 60 °C. Blends were prepared by mixing the corresponding solutions of MEH-PPV and acceptors (TNF, DNAQ, IrC_{60}, PCBM; 2–5 g/l) with their molar ratio from 1:0.01 to 1:1 per polymer monomer unit. For optical studies, films drop-cast on glass substrates were used. For photocurrent studies, sandwich-type photodiodes were prepared on indium tin oxide (ITO)-covered glass substrates. A PEDOT:PSS [poly(3,4-ethylenedioxythiophene) polystyrenesulfonate] layer was spin-cast onto the ITO-side, and then the active layer was spin-cast onto the PEDOT:PSS layer from MEH-PPV/acceptor solution at 1000–1500 rpm. After that, a top Al-electrode was deposited on the active layer.

Absorption spectra of solutions and films were measured using a fiber spectrometer or a monochromator equipped with a tungsten-halogen lamp and a silicon photodetector. For PIA spectroscopy studies, the pump beam was mechanically chopped and the PIA signal in the probe channel was

processed by a lock-in amplifier at the frequency of modulation. In the probe channel we used a tungsten-halogen lamp illuminating the sample, a monochromator, and solid-state photodetectors. As a pump source, we used a CW Nd:YAG laser (532 nm) or a diode laser (810 nm). For pristine MEH-PPV films, the PL was subtracted from the measured PIA signal. PIA data were typically obtained under nitrogen flow in the temperature range 100–300 K. The PL spectra were recorded in ambient conditions using the same set-up. In PL measurements, the pump intensity and recording time were minimal to keep the error associated with PL degradation lower than 20 %. Polymer photodiodes were illuminated in ambient conditions from the glass side by a tungsten-halogen lamp dispersed by a monochromator equipped with appropriate color filters. The optical radiation was chopped at ~70 Hz with intensity on the sample surface being less than 0.5 mW/cm^2. The preamplified photocurrent was measured by a lock-in amplifier.

RESULTS AND DISCUSSION

Intermolecular CTCs of MEH-PPV

Figure 2 shows absorption spectra of MEH-PPV/DNAQ, MEH-PPV/TNF, and pristine MEH-PPV films. It is seen that the absorption spectra of the blended films are shifted to the red by 0.1–0.2 eV and show extended absorption tails compared with the pristine MEH-PPV film. Since the optical absorption of both acceptors starts at ~3 eV, the observed optical absorption below the absorption edge of pristine MEH-PPV was assigned to the ground-state CTC (Fig. 2, inset) [22,23].

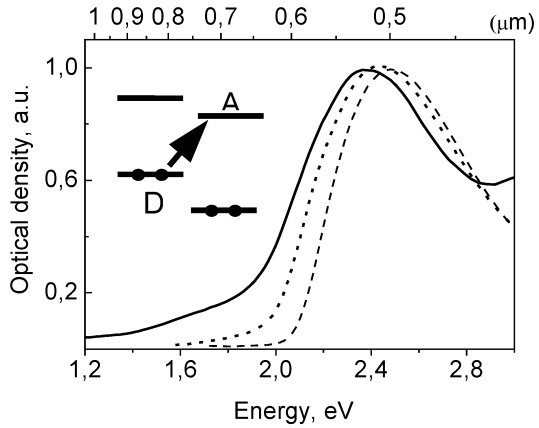

Fig. 2 Absorption spectra of pristine MEH-PPV (dashed), 1:1 MEH-PPV/DNAQ (dotted), and 1:1 MEH-PPV/TNF (solid) films drop-cast from chlorobenzene. Inset illustrates the donor and acceptor energy levels, the arrow indicates the CTC absorption corresponding to the electron transfer from the highest occupied orbital (HOMO) of the donor (D) to the lowest unoccupied orbital (LUMO) of the acceptor (A).

As TNF is a stronger acceptor (i.e., it has a higher electron affinity) than DNAQ, the CTC band should be lower in energy in the MEH-PPV/TNF blend than in the MEH-PPV/DNAQ blend according to Mulliken's model. Indeed, this is in accordance with the spectra shown in Fig. 2.

Note that the appearance of a red shift and of an extended tail in the MEH-PPV spectrum upon adding the acceptor could be associated with two other effects: enhancing intermolecular interaction of polymer chains (e.g., aggregation) and/or increasing the concentration of relatively long conjugated chains. However, since the absorption tails observed in the blends are too intense and red-shifted, it is difficult to suppose that either could result from blending.

It is natural to suggest that CTC excited states in the MEH-PPV optical gap observed as a long absorption tail play an essential role in the photophysics of the blends. To probe the photoexcited state in MEH-PPV/TNF and MEH-PPV/DNAQ blends, we used PL, PIA, and photocurrent spectroscopy techniques.

Figure 3a shows PL spectra in MEH-PPV/TNF films for different MEH-PPV:TNF molar ratio. It is seen that the PL spectra of the blends do not change their shape, corresponding to that of the pristine MEH-PPV. The same behavior was also observed in MEH-PPV/DNAQ films. Figure 3b shows the PL intensity in MEH-PPV/TNF and MEH-PPV/DNAQ blends as a function of the acceptor concentration. Note that for TNF concentration 20 % and higher, the PL was quenched by at least three orders of magnitude and was below the noise level.

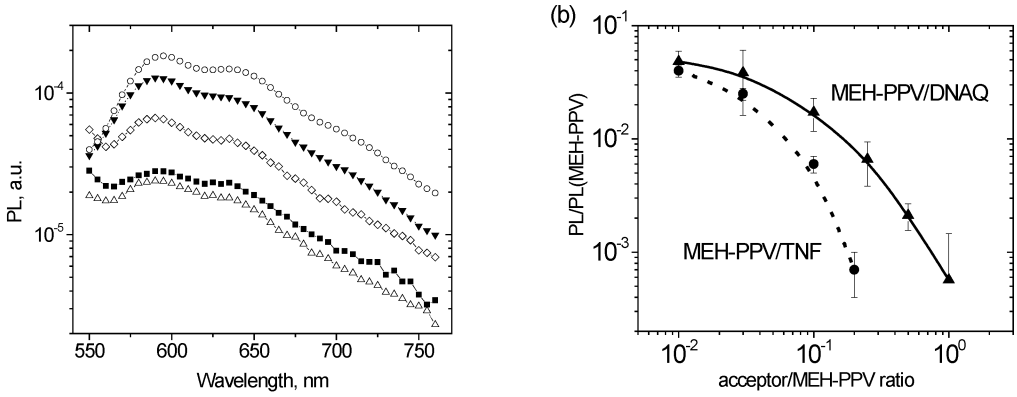

Fig. 3 PL quenching in MEH-PPV/acceptor films drop-cast from chlorobenzene. (a) Typical PL spectra for MEH-PPV/DNAQ concentration ratio 0.01, 0.03, 0.1, 0.25, and 0.5 (from top to bottom). (b) The PL intensities for TNF and DNAQ averaged on a few points on the sample, the data are normalized to the PL of pristine MEH-PPV. The lines are guides to the eye.

Our PL data show that both TNF and DNAQ are very efficient quenchers of MEH-PPV PL. PL quenching in organic donor–acceptor blends upon photoexcitation of the donor is usually indicative of either energy or charge transfer from the donor to the acceptor. Since the optical gap of DNAQ and TNF is no less than 3 eV, their optical absorption spectra do not overlap with the MEH-PPV emission spectrum. Therefore, resonance energy transfer from the MEH-PPV to the acceptor cannot be a reason for PL quenching. On the other hand, the MEH-PPV/acceptor CTC has a noticeable absorption in the optical gap of MEH-PPV, and hence the CTC could be an efficient energy funnel accumulating the MEH-PPV excitons via Forster energy transfer. Another possible mechanism of PL quenching to be analyzed is the fast photoinduced electron transfer from the MEH-PPV to the acceptor.

An important relaxation pathway of the excited CTC is generation of long-lived separated charges. PIA spectroscopy is a commonly used technique to study long-lived excited states in conjugated polymers. Absorbed photons generate neutral or charged long-lived states in the polymer that can be identified by IR bands in the PIA spectra. To probe the relaxation pathways of the low-energy excited states in the blends assigned to the CTC, we also studied PIA at IR excitation (810 nm) corresponding to the MEH-PPV optical gap. Only the CTC can be excited at this wavelength.

Figure 4 shows typical PIA spectra for pristine MEH-PPV and MEH-PPV/TNF films at low temperature for photoexcitation in the MEH-PPV absorption band at 532 nm. The most intensive peak band in the pristine MEH-PPV film is observed at 1.35 eV, and it is usually assigned to triplet states [39], while in the MEH-PPV/TNF blend the PIA spectrum was dominated by the peak band at 1.2 eV, which we associate with charged states (polarons) [40]. The different nature of peak bands at 1.2 and 1.35 eV is illustrated by their chopping frequency dependences (Fig. 4, inset). The frequency dependence for the

pristine MEH-PPV film exactly follows the monomolecular recombination kinetics, which is usually considered as a characteristic signature of triplet excitons. On the other hand, the frequency dependence for the MEH-PPV/TNF blend is close to a power function, which is usually attributed to polaron states. Moreover, the PIA signal in pristine MEH-PPV had strong temperature dependence different from that of the blend. These observations allow assignment of the PIA band at 1.2 eV observed in the blend to MEH-PPV polaron states. Remarkably, the MEH-PPV/TNF blend gives nearly the same spectra for excitation at 532 and 810 nm (Fig. 5), indicating that photoexcitation of either the MEH-PPV or the CTC results in the same charged species.

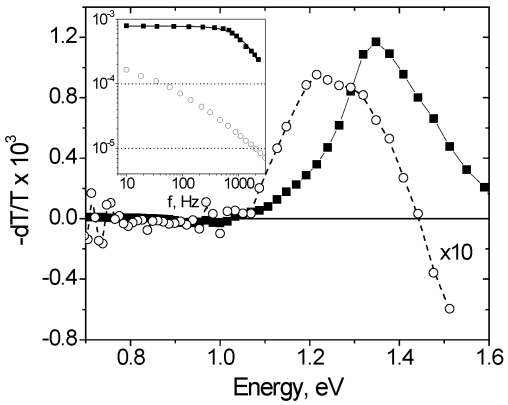

Fig. 4 PIA spectra for pristine MEH-PPV and 1:1 MEH:PPV/TNF (-) films drop-cast from cyclohexanone and recorded at 110 K for pump intensity 100 mW/cm^2 at 532 nm and chopping frequency 70 Hz. The inset demonstrates the corresponding frequency dependencies of the peak signals at 1.2 and 1.35 eV, the solid line shows a monomolecular kinetics fit for the peak at 1.35 eV.

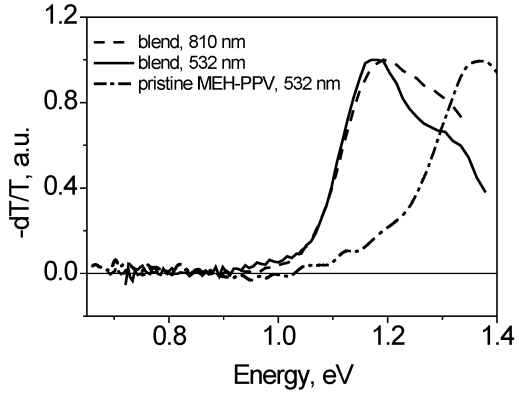

Fig. 5 Normalized PIA spectra of 1:1 MEH-PPV/TNF film drop-cast from chlorobenzene and recorded at 100 K for excitation at 532 nm (solid), 810 nm (dashes), and chopping frequency 75 Hz. PIA spectrum of pristine MEH-PPV (dash-dots) is shown for comparison.

We have found that the PIA features in MEH-PPV/TNF and MEH-PPV/DNAQ blends are very similar. Figure 6 compares the corresponding PIA data measured at pump wavelength 532 nm. These data strongly suggest that the charge generation mechanism is the same in MEH-PPV/TNF and MEH-PPV/DNAQ blends. A difference in the PIA spectra in Fig. 6 at probe energies higher than 1.4 eV could be assigned to the effect of the absorption tail, which is essentially longer for MEH-PPV/TNF

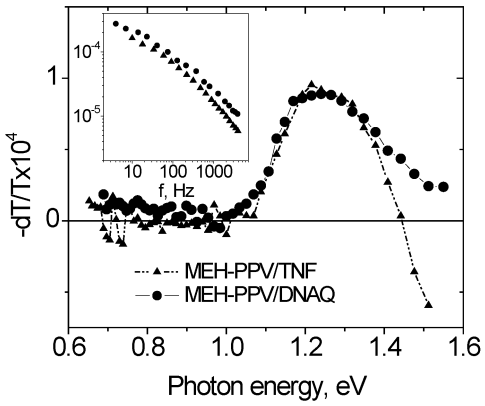

Fig. 6 PIA spectra of 1:1 MEH-PPV/DNAQ and 1:1 MEH-PPV/TNF (from Fig. 4) films prepared from cyclohexanone and chlorobenzene, respectively. The MEH-PPV/DNAQ spectrum was recorded at 110 K, pump intensity ≈0.83 W/cm^2 at 532 nm and chopping frequency 75 Hz. Inset: chopping frequency dependencies of the 1.2 eV band for the blends.

blends (Fig. 2). Indeed, bleaching the CTC excited states below the MEH-PPV absorption edge could be responsible for a negative contribution to the PIA spectrum.

Our PIA studies demonstrate that the photoexcited CTC can relax into a charged-separated state. For photovoltaics applications, an important question to be addressed is how these photoinduced charges could contribute to the photocurrent. We measured the photocurrent action spectra of photodiodes with the active layer consisting of MEH-PPV/TNF, MEH-PPV/DNAQ, and pristine MEH-PPV. The optical density of the active layer was below unity, allowing us to neglect the internal filter effect, i.e., any essential influence of the active layer thickness on the shape of the photocurrent spectra.

Figure 7 compares photocurrent action spectra of MEH-PPV/TNF, MEH-PPV/DNAQ, and MEH-PPV photodiodes. It is seen that addition of the acceptor to MEH-PPV leads to increasing the external quantum efficiency (EQE), i.e., the probability of appearance of an elementary charge at contacts per one incident photon, in the MEH-PPV optical gap. Considerable EQE increasing in the MEH-PPV optical gap with adding the acceptors is evidence for mobile charges generated in the CTC. The photocurrent action spectra in Fig. 7 correlate with the corresponding absorption spectra of the blends (Fig. 2), implying the similar charge collection efficiency over the entire investigated spectral region. At the same time, the charge collection efficiency tends to decrease with addition of TNF (Fig. 7) within

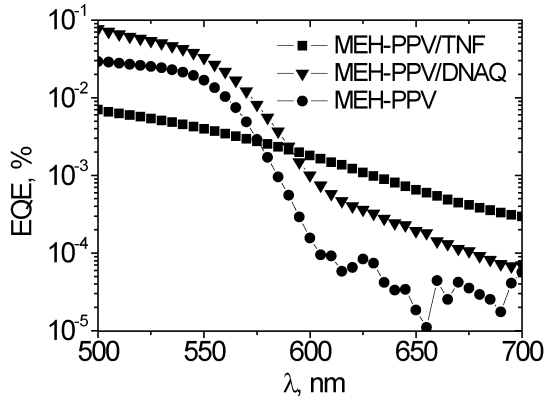

Fig. 7 Photocurrent action spectra of photodiodes with different active layers. The donor–acceptor ratio was equimolar for the blends.

the region of MEH-PPV strong absorption (~500 nm), indicating lower charge mobilities and/or higher recombination rate as compared with the pristine MEH-PPV device. On the contrary, DNAQ enhances the photocurrent in both the absorption and the transparency ranges of MEH-PPV (Fig. 7).

In summary, we have observed that the photoexcited CTC in MEH-PPV/TNF and MEH-PPV/DNAQ blends generates mobile charges. As a result, the photosensitivity spectral range of the blends is extended in the optical gap of MEH-PPV. However, the studied photodiodes with the CTC show quite low charge collection efficiencies. Possibly, the low mobility of charges in the studied blends is one of the main reasons for this behavior.

Fullerene metallocomplex

Figure 8 compares absorption spectra of IrC_{60}, PCBM, and MEH-PPV in the visible spectral range where the largest part of the solar energy spectrum is concentrated. It is seen that the molar extinction of IrC_{60} is considerably higher than that of PCBM. Remarkably, the integral absorption of IrC_{60} in the range 400–800 nm is about that of MEH-PPV as follows from the data in Fig. 8. Moreover, IrC_{60} has strong absorption in the optical gap of MEH-PPV that can significantly increase absorption of the red part of the solar spectrum by a polymer/metallofullerene blend. Supposing that the optimal polymer:metallofullerene ratio in the solar cell active layer could be about 1:1 mol/mol as for the MDMO-PPV/PCBM solar cells [25], one could expect that the enhanced absorption of metallofullerenes is able to increase the photocurrent in polymer/metallofullerene solar cells as compared with polymer/methanofullerene ones.

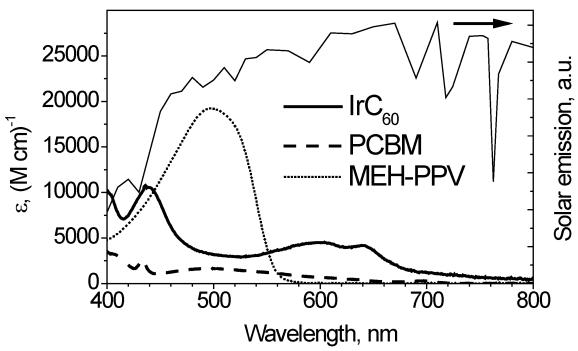

Fig. 8 Optical absorption spectra of IrC_{60} (30 μM), PCBM (200 μM), and MEH-PPV (15 μM) in toluene. Thin solid line shows the solar emission spectrum.

Photoinduced charged transfer in polymer/fullerene blends is known to occur with extremely high efficiency (about 100 %), which provides high performance of polymer/fullerene solar cells. As a result, almost every exciton photoexcited in the blend dissociates in a pair of long-lived mobile charges: the electron in the fullerene phase, and the hole in the polymer phase. To characterize the photoinduced charge-transfer reaction in MEH-PPV/IrC_{60} blends, we applied PL and PIA spectroscopies with excitation at 532 nm. We also used a well-studied MEH-PPV/PCBM system as a reference. Figure 9 shows MEH-PPV PL intensity in MEH-PPV/fullerene blended films as a function of fullerene molar concentration. It is seen that the PL quenching efficiency of IrC_{60} is about that of PCBM, indicating fast decay of the MEH-PPV exciton due to energy or charge transfer. The difference in PL quenching for acceptor concentration 0.1 could result from different fullerene aggregation in the blends. Figure 10 compares PIA spectra in MEH-PPV/IrC_{60} and MEH-PPV/PCBM blends. It is seen that the spectra in both blends are very similar and include two characteristic MEH-PPV polaron bands at 1.3 eV and below 0.6 eV. The close shape and intensity of PIA spectra observed in the MEH-PPV/IrC_{60} and MEH-PPV/PCBM

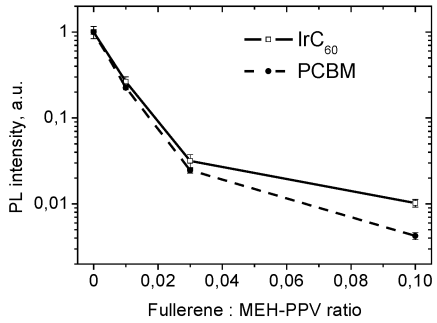

Fig. 9 MEH-PPV PL intensity in MEH-PPV/IrC_{60} and MEH-PPV/PCBM blended films drop-cast from chlorobenzene with concentration of MEH-PPV about 5 g/l.

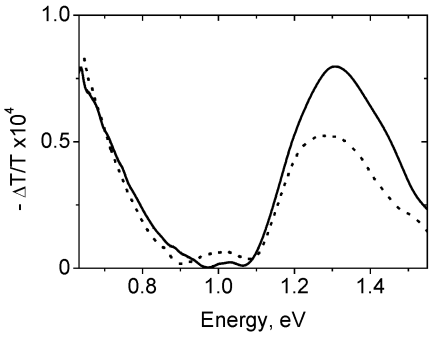

Fig. 10 PIA spectra of MEH-PPV/IrC_{60} (solid line, 1:0.1 mol/mol) and MEH-PPV/PCBM (dotted line, 1:0.1 mol/mol). The PIA spectra were recorded at room temperature for pump at 532 nm chopped at 75 Hz.

blends imply that long-lived photoinduced charges are generated in them with close efficiencies and lifetimes.

CONCLUSIONS

We have studied two types of low-bandgap materials for organic solar cells: ground-state CTCs of MEH-PPV and an exohedral metallocomplex of fullerene IrC_{60}. We have shown that the CTCs MEH-PPV/TNF and MEH-PPV/DNAQ strongly absorb light in the MEH-PPV optical gap, and the photoexcited CTCs can generate free charges. IrC_{60} demonstrates strong optical absorption in the visible spectral range that could noticeably enhance light harvesting in polymer/fullerene solar cells. Our PL and PIA data indicate that the efficiency of photoinduced charge transfer in MEH-PPV/IrC_{60} blends could be as high as in MEH-PPV/PCBM blends. Thus, our data suggest that conjugated polymer CTCs and exohedral metallofullerenes deserve further study as promising materials for organic solar cells.

ACKNOWLEDGMENTS

This work is supported by the Russian Ministry of Education and Science (contracts #02.513.11.3207 and #2.513.11.3209), Russian Foundation of Basic Research (#07-02-01227a), and by Program 3 ("Quantum macrophysics") of the Presidium of the Russian Academy of Science. We thank J. C. Hummelen for granting PCBM, V. A. Dyakov for help in sample preparation, I. V. Golovnin for absorption data in solution, and A. A. Bakulin for contributions during the early phase of this work.

REFERENCES

1. W. L. Ma, C. Y. Yang, X. Gong, K. Lee, A. J. Heeger. *Adv. Funct. Mater.* **15**, 1617 (2005).
2. J. Y. Kim, K. Lee, N. E. Coates, D. Moses, T. Q. Nguyen, M. Dante, A. J. Heeger. *Science* **317**, 222 (2007).
3. G. Li, V. Shrotriya, J. S. Huang, Y. Yao, T. Moriarty, K. Emery, Y. Yang. *Nat. Mater.* **4**, 864 (2005).
4. M. Reyes-Reyes, K. Kim, D. L. Carroll. *Appl. Phys. Lett.* **87**, 083506 (2005).
5. J. Peet, J. Y. Kim, N. E. Coates, W. L. Ma, D. Moses, A. J. Heeger, G. C. Bazan. *Nat. Mater.* **6**, 497 (2007).
6. B. Lee, V. Seshadri, H. Palko, G. A. Sotzing. *Adv. Mater.* **17**, 1792 (2005).
7. F. L. Zhang, W. Mammo, L. M. Andersson, S. Admassie, M. R. Andersson, L. Inganas, S. Admassie, M. R. Andersson, O. Ingands. *Adv. Mater.* **18**, 2169 (2006).
8. R. S. Mulliken. *J. Am. Chem. Soc.* **72**, 600 (1950).
9. R. S. Mulliken. *J. Am. Chem. Soc.* **74**, 811 (1952).
10. R. J. Sension, A. Z. Szarka, G. R. Smith, R. M. Hochstrasser. *Chem. Phys. Lett.* **185**, 179 (1991).
11. D. K. Palit, H. N. Ghosh, H. Pal, A. V. Sapre, J. P. Mittal, R. Seshadri, C. N. R. Rao. *Chem. Phys. Lett.* **198**, 113 (1992).
12. M. Ichida, T. Sohda, A. Nakamura. *Chem. Phys. Lett.* **310**, 373 (1999).
13. G. Ruani, C. Fontanini, M. Murgia, C. Taliani. *J. Chem. Phys.* **116**, 1713 (2002).
14. O. Rocquin, C. Chevrot. *Synth. Met.* **89**, 119 (1997).
15. G. Weiser. *J. Appl. Phys.* **43**, 5028 (1972).
16. P. J. Skabara, I. M. Serebryakov, I. F. Perepichka, N. S. Sariciftci, H. Neugebauer, A. Cravino. *Macromolecules* **34**, 2232 (2001).
17. S. Hotta, K. Waragai. *Synth. Met.* **32**, 395 (1989).
18. B. Xu, D. Fichou, G. Horowitz, F. Garnier. *Synth. Met.* **42**, 2319 (1991).
19. M. S. A. Abdou, F. P. Orfino, Y. Son, S. Holdcroft. *J. Am. Chem. Soc.* **119**, 4518 (1997).
20. A. A. Bakulin, S. G. Elizarov, A. N. Khodarev, D. S. Martyanov, I. V. Golovnin, D. Y. Paraschuk, M. M. Triebel, I. V. Tolstov, E. L. Frankevich, S. A. Arnautov, E. M. Nechvolodova. *Synth. Met.* **147**, 221 (2004).
21. A. A. Bakulin, A. N. Khodarev, D. S. Martyanov, S. G. Elizarov, I. V. Golovnin, D. Yu. Paraschuk, S. A. Arnautov, E. M. Nechvolodova. *Dokl. Chem.* **398**, 204 (2004).
22. D. Yu. Paraschuk, S. G. Elizarov, A. N. Khodarev, A. N. Shchegolikhin, S. A. Arnautov, E. M. Nechvolodova, *JETP Lett.* **81**, 467 (2005).
23. V. V. Bruevich, T. Sh. Makhmutov, S. G. Elizarov, E. M. Nechvolodova, D. Yu. Paraschuk. *J. Chem. Phys.* **127**, 104905 (2007).
24. S. G. Elizarov, A. E. Ozimova, D. Yu. Paraschuk, S. A. Arnautov, E. M. Nechvolodova. *Proc. SPIE* **6257**, 293 (2006).
25. H. Hoppe, N. S. Sariciftci. *J. Mater. Chem.* **16**, 45 (2006).
26. P. Panda, D. Veldman, J. Sweelssen, J. J. A. M. Bastiaansen, B. M. W. Langeveld-Voss, S. C. J. Meskers. *J. Phys. Chem. B* **111**, 5076 (2007).
27. L. Goris, K. Haenen, M. Nesladek, P. Wagner, D. Vanderzande, L. De Schepper, J. D'Haen, L. Lutsen, J. V. Manca. *J. Mater. Sci.* **40**, 1413 (2005).
28. L. Goris, A. Poruba, L. Hod'akova, M. Vanecek, K. Haenen, M. Nesladek, P. Wagner, D. Vanderzande, L. De Schepper, J. V. Manca. *Appl. Phys. Lett.* **88**, 052113 (2006).
29. J. J. Benson-Smith, L. Goris, K. Vandewal, K. Haenen, J. V. Manca, D. Vanderzande, D. D. C. Bradley, J. Nelson. *Adv. Funct. Mater.* **17**, 451 (2007).
30. M. M. Wienk, J. M. Kroon, W. J. H. Verhees, J. Knol, J. C. Hummelen, P. A. Van Hal, R. A. J. Janssen. *Angew. Chem., Int. Ed.* **42**, 3371 (2003).

31. J. L. Segura, F. Giacalone, R. Gomez, N. Martin, D. M. Guldi, C. P. Luo, A. Swartz, I. Riedel, D. Chirvase, J. Parisi, V. Dyakonov, N. S. Sariciftci, F. Padinger. *Mater. Sci. Eng., C* **25**, 835 (2005).
32. F. B. Kooistra, V. D. Mihailetchi, L. M. Popescu, D. Kronholm, P. W. M. Blom, J. C. Hummelen. *Chem. Mater.* **18**, 3068 (2006).
33. I. Riedel, E. Von Hauff, H. Parisi, N. Martin, F. Giacalone, V. Dyakonov. *Adv. Funct. Mater.* **15**, 1979 (2005).
34. L. M. Popescu, P. Van't Hof, A. B. Sieval, H. T. Jonkman, J. C. Hummelen. *Appl. Phys. Lett.* **89**, (2006).
35. P. J. Fagan, J. C. Calabrese, B. Malone. *Science* **252**, 1160 (1991).
36. F. J. Brady, D. J. Cardin, M. Domin. *J. Organomet. Chem.* **491**, 169 (1995).
37. S. A. Lerke, B. A. Parkinson, D. H. Evans, P. J. Fagan. *J. Am. Chem. Soc.* **114**, 7807 (1992).
38. M. V. Tsikalova, S. V. Zheludkov, E. V. Vorontsov, A. S. Peregudov, V. V. Bashilov, V. I. Sokolov, Y. N. Novikov. *7th Biennial International Workshop "Fullerenes and Atomic Clusters", St. Petersburg, Russia. Book of Abstracts*, p. 134 (2005).
39. D. S. Ginger, N. C. Greenham. *Phys. Rev. B* **59**, 10622 (1999).
40. X. Wei, Z. V. Vardeny, N. S. Sariciftci, A. J. Heeger. *Phys. Rev. B* **53**, 2187 (1996).